

A COMPARATIVE STUDY OF FOREST LOSS DETECTION IN LAOS USING BFAST MONITOR AND GLOBAL FOREST CHANGE DATASET

Seima Osako

MSc Geo-Information Science, Wageningen University & Research

KEY WORDS: Tropical forest, Forest monitoring, Time-series analysis, BFAST Monitor, REDD+

ABSTRACT:

In tropical zones, effective forest monitoring is critical for climate change mitigation, particularly within the context of REDD+ framework. This study assesses the accuracy of forest loss detection using a trajectory-based approach, BFAST Monitor (BFM), compared to the high-accuracy Global Forest Change (GFC) dataset in tropical regions. The study focuses on the Chomphet district in Louangphrabang province, Laos, where significant tree cover loss has occurred. Using MODIS Enhanced Vegetation Index (EVI) time-series data (2001-2023), BFM decomposes time-series data into seasonal, trend, and residual components based on a seasonal-trend model. The algorithm detects structural changes in new observations after 2020 onwards compared to the history period, with a magnitude threshold of -0.05 for forest loss classification. Results show that BFM detected 12% more forest loss than GFC, particularly identifying large-scale land use conversion patterns in the northeastern part of the study area where GFC showed limited detection capability. However, visual assessment revealed some potential overestimation by BFM in areas with partial forest conversion. This study demonstrates that BFM algorithms can effectively detect forest loss in tropical areas, but highlights the need for integration with higher resolution satellite data to more accurately distinguish between partial and complete forest loss. These findings contribute to improving forest monitoring systems, which are essential for implementing effective climate change mitigation strategies.

1. INTRODUCTION

Forest ecosystems have played a significant role in biodiversity conservation and human prosperity. However, serious deforestation has accelerated across many regions globally due to human activities, with tropical forests being particularly vulnerable. In particular, deforestation in developing countries has contributed to climate change through carbon dioxide emissions into the atmosphere. In response to these issues, Reducing Emissions from Deforestation and forest Degradation (REDD+) has been established as a critical climate change measure in the Paris Agreement. Under REDD+, developed countries provide financial support to developing countries when they successfully reduce deforestation and forest degradation or maintain/increase carbon stocks in forested areas. This measurement plays a key role not only in climate change mitigation but also in supporting local communities in developing countries through the maintenance of forest ecosystems. Laos, located in the Indochina Peninsula where forests cover the majority of the land, is one of the Southeast Asian countries facing deforestation and forest degradation. While Laos has been actively participating in forest conservation efforts through the REDD+ framework, according to the GFC dataset (Vizzuality, n.d.), from 2001 to 2023, Laos lost 4.81 Mha of tree cover, equivalent to a 25% decrease since 2000, resulting in 2.46 Gt of CO₂e emissions. Such rapid forest loss due to the artificial land use conversion from forest to non-forest causes various environmental issues including reduction in carbon stocks, decreased water resource conservation function, and loss of biodiversity. To address these environmental challenges and effectively manage forest resources, it is essential to develop accurate forest monitoring systems, although forest monitoring generally requires considerable time and effort at both global and local scales. In tropical areas, conducting multiple ground surveys is particularly challenging due to limited accessibility to

forested areas caused by poor road conditions and safety concerns. In such circumstances, remote sensing technologies, including satellite imagery, serve as indispensable tools for regular and widespread data acquisition. Indeed, the combination of remote sensing technologies and ground surveys is recommended for carbon inventory measurements (Birdsey et al., 2013) under REDD+. Therefore, developing effective tropical forest monitoring methods using remote sensing is crucial for implementing measures to mitigate deforestation and tropical forest degradation.

Forest change estimation algorithms using time-series satellite imagery can be mainly categorized into classification-based and trajectory-based approaches. As a prominent example of the classification-based approach, Hansen et al., 2013 provided a high-resolution global forest change map (GFC) using decision tree methods to estimate annual forest loss and gain from 2000 to 2012, achieving over 80% accuracy in tropical regions. In contrast, the trajectory-based approach demonstrates greater robustness against seasonal variations and outliers caused by imperfect cloud-masking processes compared to the former approach. Notably, Breaks for Additive Season and Trend (BFAST) (Verbesselt et al., 2010) excels at capturing continuous quantitative changes based on the entire time-series data and effectively detecting abrupt changes. Despite these advances, few studies have applied BFAST and directly compared these approaches in challenging tropical contexts, particularly in regions with frequent cloud cover and rapid land-use changes. This study addresses this gap by evaluating the effectiveness of these contrasting approaches in Laos, where accurate forest monitoring is crucial for REDD+ implementation.

2. RESEARCH QUESTION

This study addresses the following research questions:

- How accurate is the forest loss detection using a trajectory-based approach, BFM compared to the high-accuracy GFC based on a classification-based approach in tropical regions with frequent cloud cover?
- Are there significant differences in spatial patterns between these two approaches?

3. MATERIALS AND METHODS

3.1 Study area

In Laos, the top 6 regions were responsible for 52% of all tree cover loss between 2001 and 2023, with Louangphrabang experiencing the highest tree cover loss at 617 kha compared to an average of 267 kha (Vizzuality, n.d.). As my study area, Chomphet district in Louangphrabang province is selected (Figure 1).

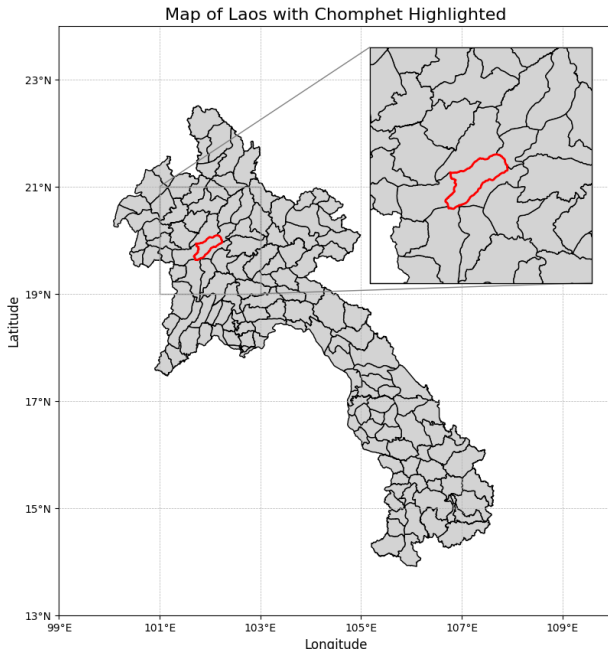


Figure 1. Map of Laos highlighting the location of "Chomphet" in red.

3.2 Satellite Data

The satellite data used in this study are summarized in Table 1. For monitoring forest changes, I utilized 16-day composite EVI (1) data with a spatial resolution of 250m, derived from the MODIS sensor for the period 2001-2023. To identify forest and non-forest areas, I used percent tree cover data from the MOD44B product at the same spatial resolution. Additionally, the Hansen GFC dataset was employed as reference data. The GFC dataset uses the year 2000 as a baseline for tree cover and monitors annual forest-to-non-forest conversion between 2000 and 2023. Accordingly, I selected the year 2000 tree cover data from MOD44B.

$$EVI = 2.5 \times (NIR - RED)NIR + 6 \times RED - 7.5 \times BLUE + 1 \quad (1)$$

Table 1. Summary: Satellite Data Used

Product Name	Band Used	Spatial Resolution	Acquisition Period
MOD13Q1.061	EVI	250m	2001-2023
MOD44B.006	PercentTreeCover	250m	2000
Hansen GFC v1.11	loss/lossyear	30m	-

3.3 Methodology

Step 1: Satellite Image Collection and Pre-processing

In the target area of Chomphet district, I collected MOD13Q1.061 EVI time-series data spanning 23 years (2001-2023), resulting in a total of 529 scenes. The MOD13Q1 product includes a SummaryQA band that indicates pixel-level data reliability. In this study, only pixels with the highest quality rating (SummaryQA = 0) can be considered as valid observations. For forest change monitoring, I restricted analysis to pixels with tree cover greater than 30% in the baseline year (2000).

Step 2: BFAST Monitor Implementation

The fundamental framework of BFAST Monitor (Verbesselt et al., 2012) is based on the decomposition of time-series data into seasonal, trend, and residual components using a seasonal-trend model. For an observation at time t , denoted as y_t , the model assumes an additive structure with a linear trend and harmonic seasonality:

$$y_t = \alpha_1 + \alpha_2 t + \sum_{j=1}^k \left[\gamma_j \sin \left(\frac{2\pi j t}{f} + \delta_j \right) \right] + \varepsilon_t \quad (2)$$

Here, α_1 represents the intercept, while α_2 is the slope representing the trend. The parameters γ_j and δ_j denote the amplitude and phase of the j -th harmonic term of the seasonal component, respectively. The frequency is represented by f (e.g., $f = 23$ for 16-day observations per year), and ε_t is the residual error term with a standard deviation σ . For this analysis, I employ the first-order harmonic model ($k = 1$) because the comparative data, GFC, is analyzed at an annual resolution. Equation (2) can be rewritten as a standard linear regression model:

$$y_t = \mathbf{x}_t^\top \boldsymbol{\beta} + \varepsilon_t \quad (3)$$

Where:

$$\begin{aligned} \mathbf{x}_t &= \{1, t, \sin\left(\frac{2\pi \cdot 1 \cdot t}{f}\right), \cos\left(\frac{2\pi \cdot 1 \cdot t}{f}\right), \dots, \sin\left(\frac{2\pi \cdot k \cdot t}{f}\right), \cos\left(\frac{2\pi \cdot k \cdot t}{f}\right)\}^T \\ \boldsymbol{\beta} &= \{\alpha_1, \alpha_2, \gamma_1 \cos(\delta_1), \gamma_1 \sin(\delta_1), \dots, \gamma_k \cos(\delta_k), \gamma_k \sin(\delta_k)\}^T \end{aligned}$$

Here:

- \mathbf{x}_t is the vector of explanatory variables, including the intercept, time, and seasonal harmonics.
- $\boldsymbol{\beta}$ is the vector of model parameters to be estimated.

Given a stable history period, determined using the Reverse Ordered Cumulative sum (ROC) approach, BFM detects structural changes in new observations using the Moving Sum (MOSUM) approach. The MOSUM statistic is defined as:

$$MO_t = \frac{1}{\hat{\sigma}\sqrt{n}} \sum_{s=t-h+1}^t (y_s - \mathbf{x}_s^\top \hat{\beta}) \quad (4)$$

Where:

- $\hat{\sigma}$: The standard deviation of the residuals.
- h : The MOSUM bandwidth, typically chosen as a fraction of the historical sample size (e.g., $h = n/4$).
- t : The time index within the monitoring period.

$|MO_t|$ exceeding a boundary corresponding to a 5% probability threshold indicates a structural change. When a structural change is detected, the magnitude of the change is estimated as:

$$\text{magnitude} = \text{median} (y_s - \mathbf{x}_s^\top \hat{\beta}), \quad s \in \text{monitoring period} \quad (5)$$

This provides a robust measure of deviation from the expected behavior modeled during the stable history period.

For this study, the historical period was defined as 2001–2019, and simulations were conducted to detect forest changes starting from January 2020. A magnitude threshold of -0.05 was applied to classify forest loss (Mashhadi & Alganci, 2022).

4. RESULTS

4.1 Quantitative Detection Comparison

Comparing forest loss detection between BFM and GFC (Figure 2), the methods identified 154.38 km^2 and 137.87 km^2 of forest loss area, respectively. While spatial patterns show general consistency between the two approaches, BFM detected 12% more forest loss area than GFC.

4.2 Spatial Pattern Analysis

The most significant difference was observed in the northeastern part of the study area where BFM identified more extensive forest loss from 2020 onwards (solid-line area in Figure 2). Analysis of EVI values comparing three-month means (January–March) between 2017 and 2023 revealed that areas detected as forest loss by BFM showed a significant decrease in EVI from 0.3–0.4 to approximately 0.1 (solid-line area in Figure 3). Historical Google Earth imagery confirmed these land use changes in the solid-line area of Figure 4. The changes in the solid-line area may be associated with mining activities, as local government reports indicate that seven mining projects and two mineral processing plants operated by Chinese investors were closed in this region in 2021 due to contract violations (Asia, 2024).

5. DISCUSSION

5.1 Detection Accuracy

The spatial pattern analysis and historical imagery validation demonstrated that BFM effectively detected major forest loss events, particularly in areas of complete land use conversion.

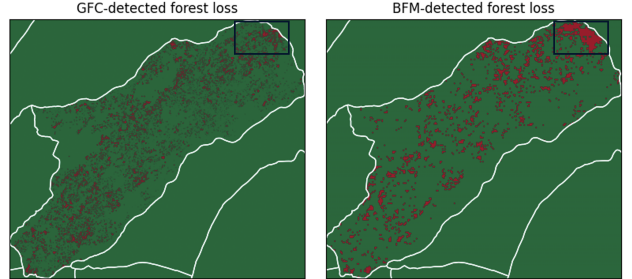


Figure 2. Forest loss in the study area as detected by GFC (left) and BFAST Monitor (right).

For comparison, Hansen et al., 2013 reported that the GFC dataset achieved over 80% User's and Producer's Accuracy in tropical regions. However, the inability to detect the large-scale land use conversion observed in my study area requires further investigation, particularly given GFC's role in meeting REDD+ guidelines for estimating forest loss and carbon dioxide emissions (Melo et al., 2023).

5.2 Method Limitations and Challenges

While examining the northeastern region where BFM identified more extensive forest loss, I found that the dotted-line area (Figure 3 and Figure 4) showed only partial forest conversion, indicating potential overestimation by BFM. This overestimation highlights the need for higher-resolution satellite data to more accurately distinguish between partial and complete forest loss.

The limited geographical scope of this study prevents definitive comparison between classification-based (GFC) and trajectory-based (BFM) approaches. Nevertheless, my findings highlight the need for continued validation of GFC accuracy and spatial pattern differences between both methods, especially in tropical regions with high carbon stocks compared to temperate and boreal zones.

6. CONCLUSIONS

This study demonstrated that forest loss detection using MODIS 250m resolution data and the BFAST Monitor algorithm achieved comparable accuracy to GFC that serves as a baseline under REDD+. Specifically, BFM detected 12% more forest loss than GFC, particularly in the northeastern part of the study area where large-scale land use conversions were identified. These findings highlight the effectiveness of BFM in capturing spatial patterns that GFC might miss. However, the study also revealed potential overestimation by BFM in areas with partial forest conversion. To address this limitation, integrating higher spatial resolution satellite imagery, such as Landsat or Sentinel-2, is essential for detecting more subtle forest disturbances. Additionally, synthetic aperture radar images that are less affected by weather conditions could further enhance the accuracy of forest loss detection in tropical forested areas.

Further investigation is needed to evaluate the effectiveness of real-time forest monitoring using BFAST Monitor in the context of forest biomass estimation and climate change mitigation. By combining multiple data sources and algorithms, more robust and accurate forest monitoring systems can be developed, contributing to the global efforts to reduce deforestation and forest degradation.

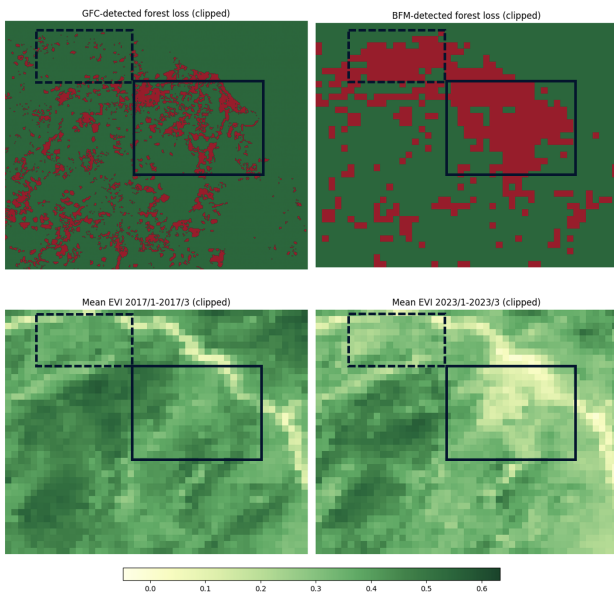


Figure 3. Comparison of forest loss and mean EVI within the northeastern part of the study area: forest loss detected by GFC (top left) and BFAST Monitor (top right); mean EVI for the periods 2017/1–2017/3 (bottom left) and 2023/1–2023/3 (bottom right).



Figure 4. Satellite imagery of the northeastern part of the study area showing changes between 5th February 2017 (left) and 2nd February 2023 (right). Source: Maxar Technologies, CNES/Airbus, Google Earth.

REFERENCES

- Asia, R. F. (2024, January). Laos to start fining mining companies amid complaints about projects. Retrieved January 22, 2025, from <https://www.licas.news/2024/01/23/laos-to-start-fining-mining-companies-amid-complaints-about-projects/>
- Birdsey, R., Angeles-Perez, G., Kurz, W. A., Lister, A., Olguin, M., Pan, Y., Wayson, C., Wilson, B., & Johnson, K. (2013). Approaches to monitoring changes in carbon stocks for REDD+. *Carbon Management*, 4(5), 519–537. <https://doi.org/10.4155/cmt.13.49>
- Hansen, M. C., Potapov, P. V., Moore, R., Hancher, M., Turubanova, S. A., Tyukavina, A., Thau, D., Stehman, S. V., Goetz, S. J., Loveland, T. R., Kommareddy, A., Egorov, A., Chini, L., Justice, C. O., & Townshend, J. R. G. (2013). High-Resolution Global Maps of 21st-Century Forest Cover Change. *Science*, 342(6160), 850–853. <https://doi.org/10.1126/science.1244693>
- Mashhadí, N., & Algancı, U. (2022). Evaluating BFASTMonitor Algorithm in Monitoring Deforestation Dynam-
ics in Coniferous and Deciduous Forests with LAND-SAT Time Series: A Case Study on Marmara Region, Turkey. *ISPRS International Journal of Geo-Information*, 11(11), 573. <https://doi.org/10.3390/ijgi11110573>
- Melo, J., Baker, T., Nemitz, D., Quegan, S., & Ziv, G. (2023). Satellite-based global maps are rarely used in forest reference levels submitted to the UNFCCC. *Environmental Research Letters*, 18(3), 034021. <https://doi.org/10.1088/1748-9326/acba31>
- Verbesselt, J., Hyndman, R., Newnham, G., & Culvenor, D. (2010). Detecting trend and seasonal changes in satellite image time series. *Remote Sensing of Environment*, 114(1), 106–115. <https://doi.org/10.1016/j.rse.2009.08.014>
- Verbesselt, J., Zeileis, A., & Herold, M. (2012). Near real-time disturbance detection using satellite image time series. *Remote Sensing of Environment*, 123, 98–108. <https://doi.org/10.1016/j.rse.2012.02.022>
- Vizzuality. (n.d.). Laos Deforestation Rates & Statistics — GFW. Retrieved January 17, 2025, from <https://www.globalforestwatch.org/dashboards/country/LAO?category=forest-change>

APPENDIX

Use of generative AI statement

I used Claude 3.5 Sonnet to improve my writing in terms of grammar mistakes and academic writing styles.

List of Acronyms

BFAST Breaks for Additive Season and Trend

BFM BFAST Monitor

EVI Enhanced Vegetation Index

GFC Global Forest Change

REDD+ Reducing Emissions from Deforestation and forest Degradation

Code availability

Code for downloading and analysis was performed using the following repository: <https://git.wur.nl/seima.osako/aoe-research-paper>